

AN INTEGRATED HUMAN AVOIDANCE AND APPROACH SYSTEM FOR MOBILE SERVICE ROBOTS IN DYNAMIC SOCIAL ENVIRONMENTS

Van Bay Hoang, Dinh Nghia Do, Lan Anh Nguyen, Van Xuan Nguyen,
Xuan Tung Truong*

Le Quy Don Technical University, 236 Hoang Quoc Viet, Bac Tu Liem, Ha Noi, Viet Nam

*Emails: xuantung.truong@gmail.com

Received: 6 April 2021; Accepted for publication: 10 November 2021

Abstract. In this study, we present a socially aware navigation framework for mobile service robots by integrating the systems proposed in our previous studies into a completed mobile robot navigation system, including the human detection and tracking system that is used to detect and track humans; the encoder and laser-based localization and mapping system that is used to determine the position of the robot in the environment; the approaching pose estimation system that is used to estimate the approaching pose of the robot to the human; and the social timed elastic band-based motion planning system that is used to socially navigate the mobile robots to approach the human. In addition, in the paper we describe in detail the motor control system and the design of our mobile robot platform, which is then utilized to conduct experiments in the real-world environments. We verify the feasibility and usefulness of the proposed socially aware robot navigation framework through a series of experiments in a corridor-like environment. The experimental results show that our proposed framework is able to drive the mobile robots to both avoid and approach the humans, providing the safety and comfort for the humans and socially acceptable behaviors for the mobile service robots in the dynamic social environments.

Keywords: Socially aware navigation framework, mobile service robot, approaching human, timed elastic band technique, motion planning system.

Classification numbers: 2.4.2, 2.4.4, 5.2.1.

1. INTRODUCTION

Dynamic social environments are unstructured, clustered, dynamic and uncertain environments with the presence of humans, vehicles and even other autonomous devices. Therefore, in order to autonomously and safely navigate in such environments, the most important issue is that the mobile robots must avoid not only regular obstacles, but also dynamic humans during the navigation process. To this end, several socially aware navigation frameworks have been developed for the mobile robots in the dynamic social environments [1 - 3].

The conventional socially aware navigation frameworks can be divided into two groups based on the robot navigation tasks: (i) avoiding human framework and (ii) approaching human framework. In the former, the authors developed socially aware navigation frameworks, which enable the mobile robots to safely and socially avoid the humans and human groups in dynamic

social environments, providing the safety and comfort for the surrounding humans. Whereas, in the later, the conventional navigation frameworks allow the mobile robots to approach a human or human group, allowing the socially acceptable approaching behaviors.

Several navigation frameworks, which enable the mobile robots to safely and socially avoid humans, have been developed in recent years [4 - 8]. Although these approaches have been successfully applied in real-world environments, most of the conventional frameworks did not take into account the motion dynamics of the mobile robots, including the kinodynamic constraints, the limitations of the velocity and acceleration, therefore the frameworks might be difficult to be directly applied in a real-world environment. As a result, such developed navigation systems lack robustness in dynamic social environments.

Recently, a number of conventional human approaching frameworks, which allow the mobile robots to approach a single person [9, 10] or a group of people [11, 13] have been recently proposed. Some of these human approaching systems have been implemented and verified on mobile platforms to illustrate the viability of generating socially acceptable approaching behaviors for the mobile robots. However, most of these methods have only been implemented and validated in simulation environments.

In this study, we present an integrated socially aware navigation framework for mobile robots by incorporating the techniques proposed in our previous studies, including human detection and tracking, encoder and laser-based localization and mapping, approaching pose estimation, and social timed elastic band-based motion planning systems into a completed navigation framework. The proposed navigation framework takes into account both robot dynamics and the estimated approaching pose. Therefore, it enables the mobile robots to both approach and avoid the humans, providing the safety and comfort for the human in the vicinity of the robots.

The remainder of the paper is organized as follows. Section 2 presents the proposed integrated socially aware navigation framework. The experimental results in real-world environments are described in Section 3. We provide the conclusion of the paper in Section 4.

2. PROPOSED NAVIGATION FRAMEWORK

2.1. The Problem Description



Figure 1. An example of a dynamic social environment including a mobile robot and three people: (a) third person view, (b) robot's field of view. The mobile robot is requested to approach a group of people while avoiding another moving person.

We consider a dynamic social environment with the presence of a mobile robot and N humans in the robot's vicinity, as shown in Fig. 1.

The robot is requested to navigate from the initial state $s_r^s = [x_r^s, y_r^s, \theta_r^s, v_r^s, \omega_r^s]^T$ to approach a person or a group of people, while safely and socially avoiding other humans during the navigation process, where $[x_r^s, y_r^s]^T$ is the initial position, θ_r^s is the initial orientation, v_r^s is the initial linear velocity, and ω_r^s is the initial angular velocity of the robot. We assume the robot state at the time k $s_r^k = [x_r^k, y_r^k, \theta_r^k, v_r^k, \omega_r^k]^T$, where $[x_r^k, y_r^k]^T$ is the position, θ_r^k is the orientation, v_r^k is the linear velocity, and ω_r^k is the angular velocity. We also assume that there are N people appearing in the vicinity of the robot $P = \{p_1, p_2, \dots, p_N\}$, where p_i is the i^{th} person. The state of the person p_i is represented as $s_p^i = [x_p^i, y_p^i, \theta_p^i, v_p^i]^T$, where $[x_p^i, y_p^i]^T$ is the position, θ_p^i is the orientation, and v_p^i is the linear velocity. The radius of the robot and human are r_r and r_h , respectively.

2.2. The Architecture of Navigation Framework

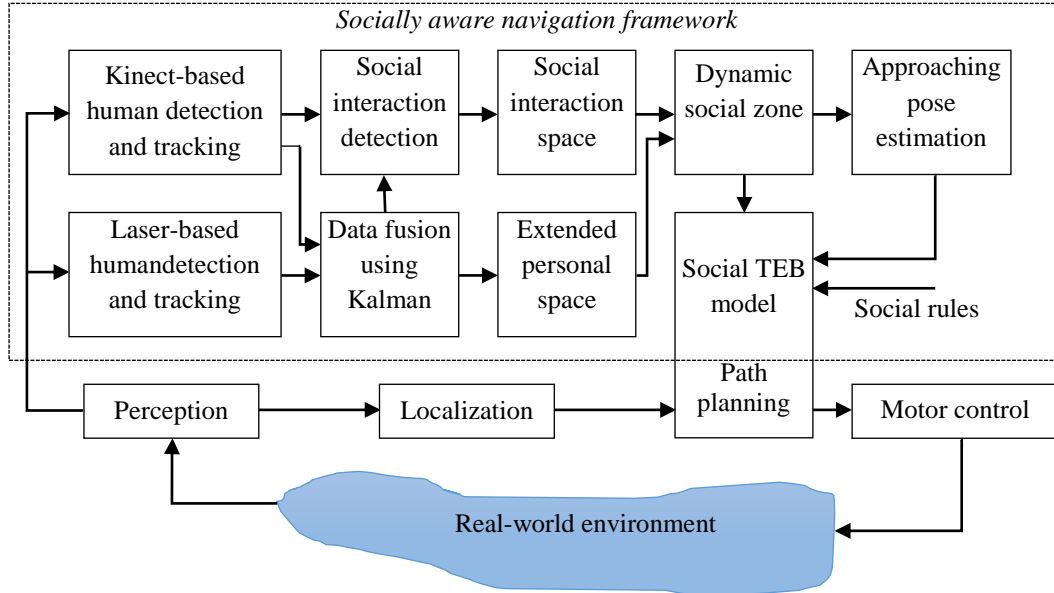


Figure 2. The block diagram of the mobile robot navigation system.

Our objective in this study is to develop a navigation framework that enables a mobile robot to autonomously, safely and socially avoid and approach humans in dynamic social environments. To achieve that goal, we propose an efficient mobile robot navigation framework based on the conventional navigation framework presented in [14], as shown in Fig. 2. This social navigation framework consists of two major parts: (i) the conventional navigation scheme, and (ii) the socially aware navigation framework (in the dash line box). In the first part, the conventional navigation scheme is based on the composition of four typical functional blocks: perception, localization, motion planning, and motor control. In the extended part, the socially aware navigation framework aims at distinguishing the humans from regular obstacles by extracting their socio-spatio-temporal characteristics in the robot's vicinity for the development of the approaching pose estimation of the robot to a human or a group of humans, and the social

timed elastic band model. Specifically, a laser-based human detection and tracking function is used to detect and track humans in the real-world environment using laser data, while a Kinect-based human detection and tracking function is used to detect and track human using data from Kinect. Once the human states including position, orientation and motion are extracted and the social interactions including human groups and human-object interactions are detected, a dynamic social zone (DSZ) is consequently generated around the humans. The DSZ is then used as the input of the approaching pose estimation function, which generates the approaching pose of the robot to the people. The DSZ and the estimated approaching pose are then used as inputs to the social timed elastic band model, which generates the motion control command for the mobile robot.

2.3. Perception System

To avoid and approach humans in dynamic social environments, the mobile robot needs to detect and track humans in its vicinity. In this paper, we used two human detection and tracking algorithms according to the data used as inputs of the systems, including laser-based and Kinect-based techniques. The laser-based system is utilized to detect and track the human using the laser data, while the Kinect-based system is made use of to estimate the 3D pose of the humans, which is then utilized to estimate the social interactions. It is noted that, the humans detected by the Kinect are also the humans which the mobile robot would like to approach.

In this study, we use the laser-based human detection algorithm developed in [15] to detect the human in the robot's vicinity, we then use the Kalman filter [16] to estimate the position and velocity of the surrounding humans. In addition, we apply the results from a previous research [17] to get the 3D pose of the humans, which is then used as input of the social interaction detection algorithm proposed by Truong *et al.* [11], as shown in Fig. 2. Furthermore, to improve the performance of the perception system we fuse the outputs of the laser-based human detection system and Kinect-based system using Kalman filter [16], as seen in Fig. 2. As a result, the output of the perception system is the human states including human's position, orientation and velocity, and the social interaction information. These informations are then used as the input of the next system, as seen in Fig. 2. An example result of the perception system is shown in Fig. 3, in which the laser-based human detection algorithm can detect 3 people, while the Kinect-based system can detect two standing people in the field of view of the Kinect sensor.

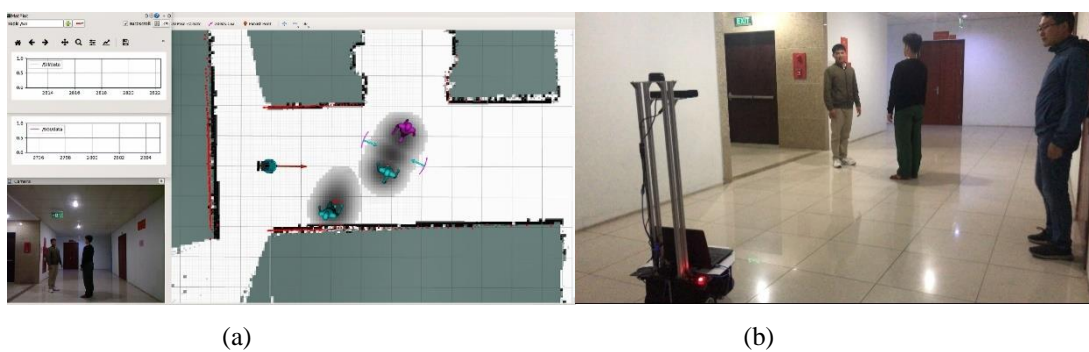


Figure 3. The example result of the perception system: (a) the screenshot of the RViz environment, and (b) the third person view.

2.4. Localization and Mapping System

In order to autonomously navigate in a dynamic real-world environment, the mobile robot should be able to determine its pose related to the surrounding environment. To accomplish that, we adopted the localization technique proposed in [18], then utilized the mapping technique presented in [19].

To determine the pose of the mobile robot, we use the encoder of the left and right wheels. To do that, we assume e_l and e_r are the resolution of the left and right encoders, respectively; Δ_e^l and Δ_e^r are number of encoder stick of left and right encoders in a time interval Δ_t ; Δ_p^l and Δ_p^r are the positions of left and right wheels in radian, and calculated as follows:

$$\Delta_p^l = \Delta_e^l 2\pi / k_m e_l \quad (1)$$

$$\Delta_p^r = \Delta_e^r 2\pi / k_m e_r \quad (2)$$

where, k_m is the gear ratio of the motor. We also assumed d_w^l and d_w^r are the travel distances of the left and right wheels, respectively, and calculated as follows:

$$d_w^l = \Delta_p^l r_w^l w_r^l \quad (3)$$

$$d_w^r = \Delta_p^r r_w^r w_r^r \quad (4)$$

where, r_w^l, r_w^r are the radius of the left and right wheels, respectively; w_r^l and w_r^r are the weights for the left wheel radius and right wheel radius, respectively. Assume Δ_x, Δ_y and Δ_θ are the distances that the mobile robot has traveled along the x, y axes and robot direction in a time interval Δ_t , respectively.

$$\begin{bmatrix} \Delta_x \\ \Delta_y \\ \Delta_\theta \end{bmatrix} = \begin{bmatrix} d_s \cos(\theta + \Delta_\theta / 2) \\ d_s \sin(\theta + \Delta_\theta / 2) \\ (d_w^l - d_w^r) / d_w w_w \end{bmatrix} \quad (5)$$

where, $d_s = (d_w^l + d_w^r) / 2$ is the traveled distance of the center of the robot; d_w and w_w are the wheel separation and the weight for the wheel separation, respectively. The following equations are used to determine the odometry of the mobile robot.

$$\begin{bmatrix} x_r^{k+1} \\ y_r^{k+1} \\ \theta_r^{k+1} \end{bmatrix} = \begin{bmatrix} x_r^k \\ y_r^k \\ \theta_r^k \end{bmatrix} + \begin{bmatrix} \Delta_x \\ \Delta_y \\ \Delta_\theta \end{bmatrix} \quad (6)$$

$$\begin{bmatrix} \dot{x}_r^k \\ \dot{y}_r^k \\ \dot{\theta}_r^k \end{bmatrix} = \begin{bmatrix} \Delta_x / \Delta_t \\ \Delta_y / \Delta_t \\ \Delta_\theta / \Delta_t \end{bmatrix} \quad (7)$$

where, (x_r^k, y_r^k) and θ_r^k are the position and direction of the robot at the time k, respectively; $\dot{x}_r^k, \dot{y}_r^k, \dot{\theta}_r^k$ are the velocity that the mobile robot has traveled along the x, y axes and the orientation θ , respectively.

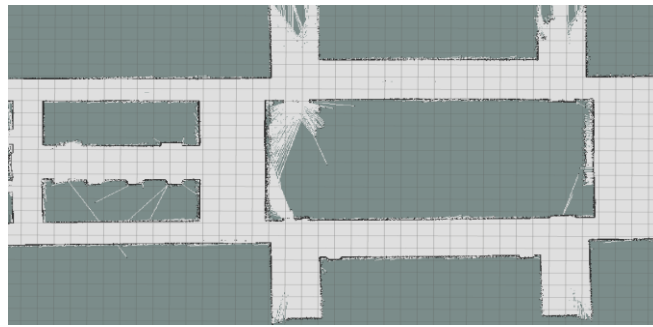


Figure 4. The result of the localization and mapping system.

The odometry is then fused with the IMU signal to generate the accurate pose of the mobile robot using the localization algorithm proposed in [18]. We then utilized the mapping technique presented in [19] to generate the map, as seen in Fig. 4, using the odometry and the laser data.

2.5. Motion Planning System

To safely and socially avoid and approach humans in dynamic social environments, in this paper we utilize approaching pose estimation method presented in [11], A* path planning algorithm described in [20] and social timed elastic band (STEB) technique proposed in [7].

2.5.1. Approaching Pose Estimation Method

In order to approach a human or human group, a mobile robot should be capable of estimating an approaching pose of the robot to the human or human group. To accomplish that, in this study, we first model the space around the human and human group using the dynamic social zone model, which contains the social interaction space [21] and the extended personal space [22], as presented in Fig. 2 and in [11]. We then utilize the approaching pose estimation algorithm proposed in [11] to estimate a proper approaching pose of the mobile robot to the human or human group. Example results are illustrated in Fig. 3, in which the gray area around the humans represents the dynamic social zone, and the output of the approaching pose estimation algorithms is two magenta arrows next to the group of two standing people, corresponding to the two potential approaching poses. Then, the mobile robot will select the approaching pose close to its current position.

2.5.2. Path Planning Algorithm

In this paper, the A* path planning algorithm [20] is adopted for finding the global path from the initial position to the approaching pose of the mobile robot. It is one of the most popular choices for path planning, because it is fairly simple and flexible. This algorithm considers the map as a two-dimensional grid with each tile being a node or a vertex. And it is based on graph search methods and works by visiting vertices (nodes) in a graph starting with the current position of the robot all the way to the goal. The key to the algorithm is identifying the appropriate successor node at each step.

Given the information regarding the goal node, the current node, and the obstacle nodes, we can make an educated guess to find the best next node and add it to the list. A* algorithm uses a heuristic algorithm to guide the search while ensuring that it will compute a path with minimum

cost. It calculates the distance (also called the cost) between the current location in the workspace, or the current node, and the target location. It then evaluates all the adjacent nodes that are open (i.e., not an obstacle nor already visited) for the expected distance or the heuristic estimated cost from them to the target, also called the heuristic cost $h(n)$. It also determines the cost to move from the current node to the next node, called the path cost $g(n)$. Thus, the total cost to get to the target node $f(n) = h(n) + g(n)$ is computed for each successor node and the node with the smallest cost is chosen as the next point.

2.5.3. Social Timed Elastic Band Technique

Timed elastic band (TEB) is an online trajectory planning algorithm for online collision avoidance, and has been successfully applied in dynamic environments [23 - 25]. The advantages of the TEB technique is that, it takes into account the robot dynamics including kinodynamic constraints, limitations of the velocity and acceleration. In addition, the technique is able to transit between obstacles in dynamic social environments. In our previous paper [7], we proposed a social timed elastic band (STEB) model, which enables a mobile robot to avoid humans in socially acceptable behaviors. The main idea of the proposed STEB model is to incorporate the social rule of avoiding the human on the right into the conventional TEB technique. The output of the STEB model is the motion control command of the mobile robot $\mathbf{u}_r = [v_r, \omega_r]$. Using the STEB model, we expected that the mobile robot equipped with the STEB model is able to socially and safely avoid and approach the humans in dynamic social environments. An example result of the motion planning system is presented in Fig. 5, in which the mobile robot avoids the human on the right-hand side.

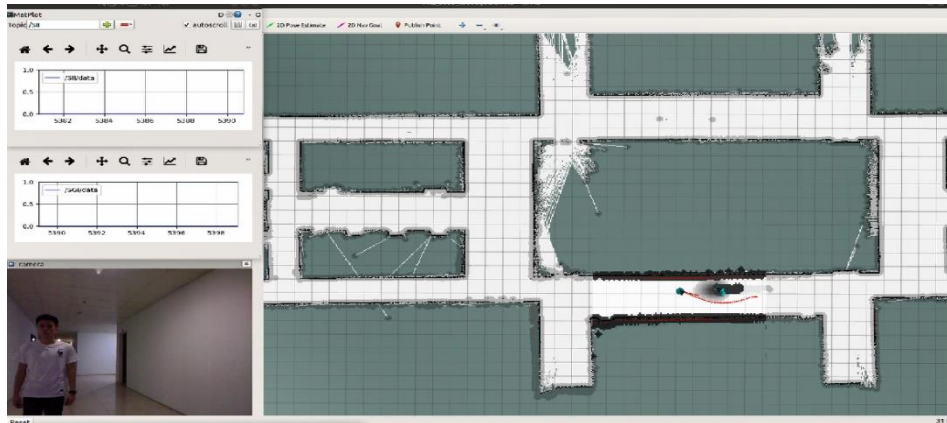


Figure 5. The example result of the motion planning system. The red curve is the robot's trajectory generated by the STEB algorithm.

2.6. Motor Control System

Once the socially optimal trajectory is generated by the STEB algorithm, the motion control command $\mathbf{u}_r = [v_r, \omega_r]$ is extracted and utilized to drive the mobile robot to avoid the humans and regular obstacles in the robot's vicinity and approach the estimated approaching pose. In this study, we utilize a two-wheel differential drive mobile robot platform to conduct the experiments. Therefore, the following equations are used to calculate the linear velocity commands v_r^l and v_r^r of the left and right wheels of the mobile robot, respectively.

$$v_r^l = (v_r - \omega_r w_w d_w / 2.0) / w_r^l r_w^l \quad (8)$$

$$v_r^r = (v_r + \omega_r w_w d_w / 2.0) / w_r^r r_w^r \quad (9)$$

where, v_r and ω_r are the linear and angular velocities generated by the STEB model, respectively. It is noted that, we utilize the aforementioned weights to tune the values of the components because of the mechanical design error.

In this study, we used a powerful driver module for controlling the DC servo motor [27]. The driver module had a PID control algorithm installed. In addition, the company also provided a software for auto-tuning the parameters of PID control algorithm. The input control command of the driver module ranges from 0 to 255. Therefore, the motion control commands of the wheels v_r^l and v_r^r are mapped to other ranges of values using the following equations:

$$v_r^l = \begin{cases} w_f^l v_r^l + T_v & \text{if } v_r^l > 0 \\ w_b^l v_r^l - T_v & \text{if } v_r^l < 0 \end{cases} \quad (10)$$

$$v_r^r = \begin{cases} w_f^r v_r^r + T_v & \text{if } v_r^r > 0 \\ w_b^r v_r^r - T_v & \text{if } v_r^r < 0 \end{cases} \quad (11)$$

where, v_r^l and v_r^r are the new motion control commands of the left and right wheels, respectively; w_f^l and w_b^l are the weights for the forward and backward movements, respectively; T_v is the minimum value that the driver allows the mobile robot starting to move. The v_r^l and v_r^r values are then sent to the driver module using RS-232 serial communication.

3. EXPERIMENTS

We have implemented and installed the proposed socially aware navigation framework on our mobile robot platform, as shown in Fig. 6(b), to validate its feasibility and effectiveness. The value of parameters of the proposed framework is empirically set as shown in Table 1.

Table 1. Parameters set in experiments.

Parameter	Value	Parameter	Value	Parameter	Value
d_w	0.335 (m)	r_w^l	0.0762 (m)	w_r^l	1.003
e_l	500 CPR	r_w^r	0.0762 (m)	w_r^r	1.0
e_r	500 CPR	r_r	0.25 (m)	w_f^l	17.5779
k_m	27	r_h	0.25 (m)	w_b^l	24.3597
T_v	20	Δ_t	0.1 (s)	w_w	1.0

3.1. Mobile Robot Platform

In a real-world environment, we used a mobile robot platform equipped with a Microsoft Kinect sensor and a laser rangefinder, as shown in Fig. 6(b). The Kinect sensor composed of a depth sensor and a RGB camera was positioned at a height of 1.1 m from the ground. The depth sensor range is from 0.8 m to 6.0 m with a vertical viewing angle of 43° and a horizontal viewing angle of 57° . This low-cost hardware can provide RGB-D data with 640×480 pixels resolution at a maximal frame rate of 30 frames per second. The laser rangefinder, Rplidar A2M8, positioned at a height of 1.2 m provides distance measurements up to 12.0 m in an angular field of view of 360° . A detailed description of the hardware components of the robot platform is shown in Fig. 7. We use the planetary DC servo motor equipped with the encoder that has 500 counts per revolution (CPR) [26]. In addition, we also make use of a powerful driver module for controlling the DC servo motor [27].

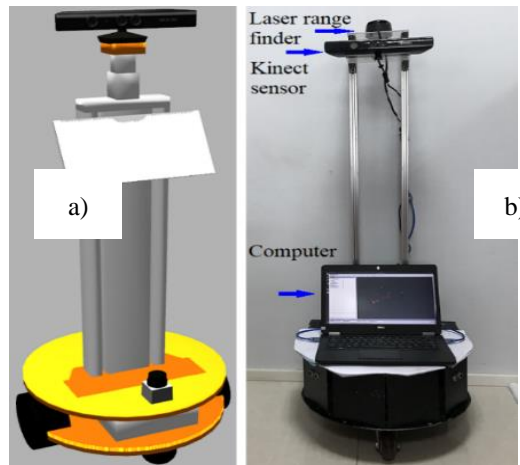


Figure 6 (a). The 3D model of the mobile robot; (b) The used mobile robot platform equipped with the Kinect sensor and laser rangefinder.

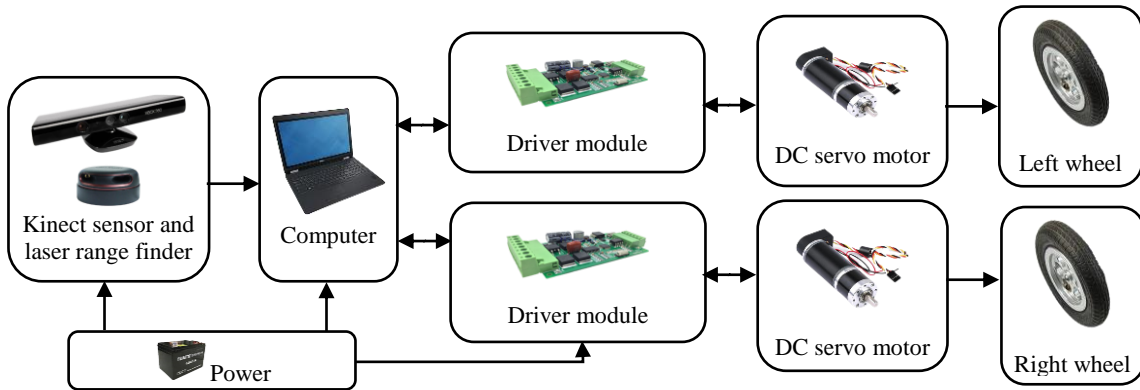


Figure 7. The hardware block diagram of the used mobile robot platform.

3.2. Experimental Setup

In this paper, we use a mobile robot platform equipped with a laser rangefinder and a Kinect sensor, as shown in Fig. 6(b). The laser rangefinder is used for robot localization and detecting humans in the vicinity of the mobile robot. The Kinect sensor is used for detecting the

humans who the robot would like to approach. The software of the proposed framework is designed and implemented using the C/C++ and Python programming language. The entire socially aware navigation framework is developed based on the Robot Operating System (ROS) [28] and run on an Intel core i7 2.7 GHz laptop. The conventional TEB package [29] was inherited and modified for developing the proposed framework. To evaluate the proposed framework, we utilize the social individual index (SII) and the social group index (SGI) proposed in [11]. These indices are used to estimate the human safety and comfort and socially acceptable behaviors of the mobile robot. Specifically, the SII value is applied to measure the physical safety and psychological safety of each individual, whereas the SGI value is used to measure the comfortable safety of the human group. The behavior of the mobile robot is considered as comfort if the SII and the SGI values are smaller than the threshold $T_c = 0.14$ and $T_g = 0.14$, respectively. Meanwhile, it is physical safety if the SII value is between the threshold $T_c = 0.14$ and $T_p = 0.54$. The mobile robot crashes into the person or crosses the interaction space between members in the human group, if the SII and SGI values are greater than the threshold $T_p = 0.54$.

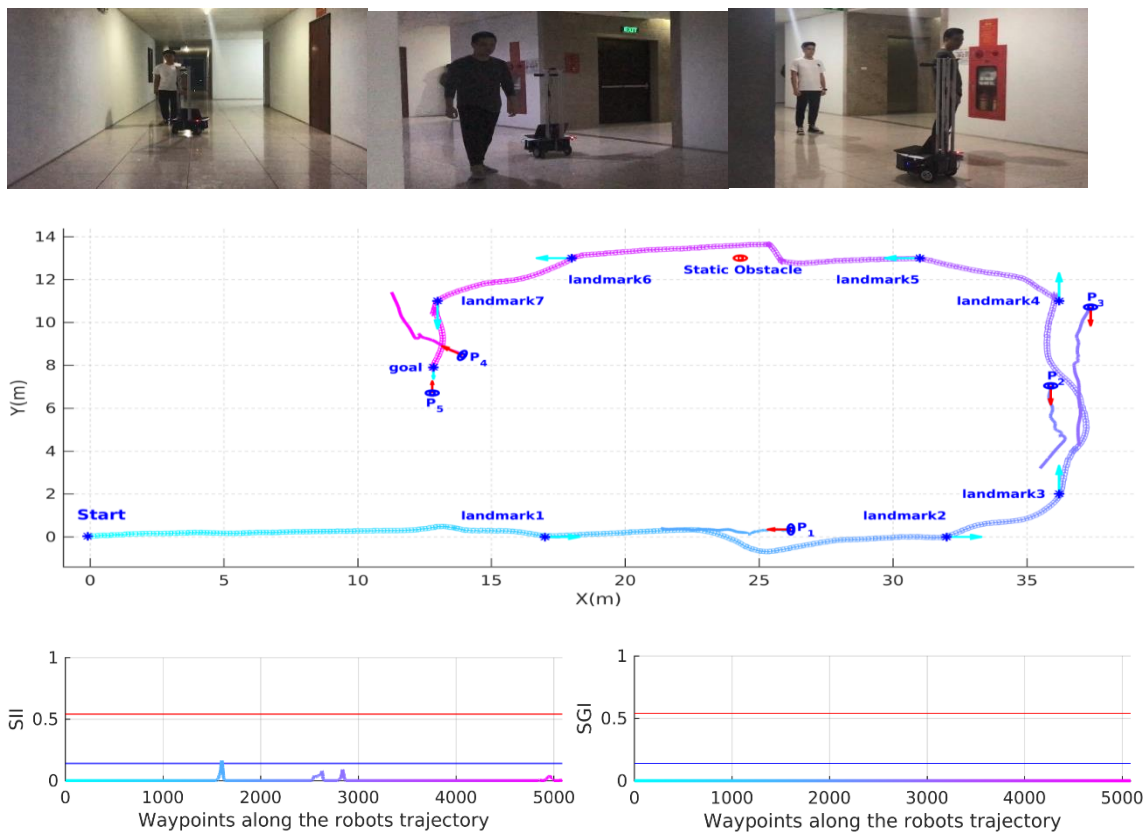


Figure 8. The results of the experiments: The first row shows snapshots of the experiments; the second row illustrates the trajectories of the mobile robot and the humans; and the final row represents the social individual index (SII) and social group index (SGI) values, respectively.

We conducted an experiment in a corridor-like environment to examine whether our mobile robot platform equipped with the proposed framework could safely and socially approach and avoid dynamic humans. In this experiment, the mobile robot is requested to navigate around the

corridor using 7 landmarks. The robot is required to avoid four moving people, a stationary obstacle, and finally approach a standing person.

3.3. Experimental Results

The experimental results are shown in Fig. 8, in which the first row shows scenario's snapshots of the experiments, while the second row illustrates the trajectories of the mobile robot and the humans, and the last row represents the SII and SGI values.

The second row of Fig. 8 illustrates that the mobile robot successfully avoids dynamic moving humans and approaches a standing person. As can be seen from the final row of Fig. 8, the SII and SGI values are smaller than the threshold T_c and T_g , respectively, indicating that the mobile robot always maintains safe and comfortable distances to the human and human group. As a result, the mobile robot equipped with the proposed framework is able to safely avoid the dynamic moving humans and socially approach another person. A video with our experimental results can be found at our link given in [30].

4. CONCLUSIONS AND DISCUSSION

We have proposed an integrated socially aware navigation framework for a mobile robot by incorporating the techniques proposed in our previous studies, including human detection and tracking, encoder and laser-based localization and mapping, approaching pose estimation, and social timed elastic band-based motion planning systems into a completed navigation system. In addition, we describe in detail the design of our mobile robot platform, which is used to conduct experiments in a real-world environment. We verify the feasibility and usefulness of the proposed framework through a series of experiments in a corridor-like environment. The experimental results show that our proposed framework is able to drive the mobile robot to both safely and socially avoid and approach people.

In the future, we will apply powerful deep learning techniques [31 - 32] for predicting human movements and trajectories in the robot's surrounding environments and incorporate this information into the proposed mobile robot navigation framework.

***CRedit* authorship contribution statement.** Van Bay Hoang and Xuan Tung Truong are proposed the system. Dinh Nghia Do, Lan Anh Nguyen and Van Xuan Nguyen are conducted the experiments.

Declaration of competing interest. This research is funded by Vietnam National Foundation for Science and Technology Development (NAFOSTED) under grant number 102.01-2018.10.

REFERENCES

1. Kruse T., Pandey A. K., Alami R., and Kirsch A. - Human-aware robot navigation: A survey, *Robotics and Autonomous Systems* **61** (2013) 1726-1743.
2. Rios-Martinez J., Spalanzani A., and Laugier C. - From proxemics theory to socially-aware navigation: A survey, *International Journal of Social Robotics*, September 2014.
3. Christoforos M., Francesca B., Allan W., Dapeng Z., Pete T., Aaron S., and Jean O. - Core challenges of social robot navigation: A survey, "arXiv:2103.05668v2, 2021, pp. 1-28.

4. Shiomi M., Zanlungo F., Hayashi K., and Kanda T. - Towards a socially acceptable collision avoidance for a mobile robot navigating among pedestrians using a pedestrian model, *International Journal of Social Robotics* **6** (3) (2014) 443-455.
5. Chen Y. F., Everett M., Liu M., and How J. P. - Socially aware motion planning with deep reinforcement learning, In: *IEEE/RSJ International Conference on Intelligent Robots and Systems*, September 2017, pp. 1343-1350.
6. Truong X. T. and Ngo T. D. - Toward socially aware robot navigation in dynamic and crowded environments: A proactive social motion model, *IEEE Transactions on Automation Science and Engineering* **14** (4) (2017) 1743-1760.
7. Hoang V. B., Nguyen V. H., Nguyen L. A., Quang T. D., and Truong X. T. - Social constraints-based socially aware navigation framework for mobile service robots, In: *Proceedings of the 7th Nafosted Conference on Information and Computer Science (NICS)*, 2020, pp. 84-89.
8. Fan T., Long P., Liu W., and Pan J. - Distributed multi-robot collision avoidance via deep reinforcement learning for navigation in complex scenarios, *The International Journal of Robotics Research* **39** (7) (2020) 856-892.
9. Trinh T. Q., Wengefeld T., Mueller S., Vorndran A., Volkhardt M., Scheidig A., and Gross H. - Take a seat, please: Approaching and recognition of seated persons by a mobile robot, In: *50th International Symposium on Robotics*, June 2018, pp. 1-8.
10. Mizumaru K., Satake S., Kanda T., and Ono T. - Stop doing it! approaching strategy for a robot to admonish pedestrians, In: *14th ACM/IEEE International Conference on Human-Robot Interaction*, March 2019, pp. 449-457.
11. Truong X. T. and Ngo T. D. - To Approach Humans?: a unified framework for approaching pose prediction and socially aware robot navigation, *IEEE Transactions on Cognitive and Developmental Systems* **10** (3) (2017) 557-572.
12. Yang F. and Peters C. - App-1stm: Data-driven generation of socially acceptable trajectories for approaching small groups of agents, In: *Proceedings of the 7th International Conference on Human-Agent Interaction*, 2019, pp. 144-152.
13. Nguyen V. H., Hoang V. B., My C. A., Kien L. M., and Truong X. T. - Toward socially aware trajectory planning system for autonomous mobile robots in complex environments, In: *Proceedings of the 7th Nafosted Conference on Information and Computer Science (NICS)*, 2020, pp. 90-95.
14. Siegwart R., Nourbakhsh I. R., and Scaramuzza D. - *Introduction to Autonomous Mobile Robots*. The MIT Press, February 2011.
15. Arras K. O., Mozos O. M., and Burgard W. - Using boosted features for the detection of people in 2d range data,” in *IEEE International Conference on Robotics and Automation*, April 2007, pp. 3402-3407.
16. Welch G. and Bishop G. - *An Introduction to the Kalman Filter*. Chapel Hill, NC, USA: Tech. Rep. TR-95-041, University of North Carolina at Chapel Hill, 2006.
17. PrimeSense NITE, <http://www.openni.org>. Accessed 6 August 2012.
18. Nguyen L. A., Dung P. T., Ngo T. D., and Truong X. T. - Improving the accuracy of the autonomous mobile robot localization systems based on the multiple sensor fusion methods, In: *International Conference on Recent Advances in Signal Processing, Telecommunications Computing*, 2019, pp. 33-37.

19. Giorgio Grisetti, Cyrill Stachniss, and Wolfram Burgard - Improved Techniques for Grid Mapping with Rao-Blackwellized Particle Filters, *IEEE Transactions on Robotics* **23** (2007) 34-46.
20. Hart P. E., Nilsson N. J., and Raphael B. - A formal basis for the heuristic determination of minimum cost paths, *IEEE Transactions on Systems Science and Cybernetics* **4** (2) (1968) 100-107.
21. Kendon A. - *Conducting interaction: Patterns of behavior in focused encounters*, Cambridge University Press, 1990.
22. Hall E. T. - *The hidden dimension: man's use of space in public and private*, The Bodley Head Ltd, London, 1996.
23. Rosmann C., Feiten W., Wosch T., Hoffmann F., and Bertram T. - Trajectory modification considering dynamic constraints of autonomous robots, In: 7th German Conference on Robotics, May 2012, pp. 1-6.
24. Rosmann C., Hoffmann F., and Bertram T. - Integrated online trajectory planning and optimization in distinctive topologies, *Robotics and Autonomous Systems* **88** (2017) 142-153.
25. Rosmann C., Oeljeklaus M., Hoffmann F., and Bertram T. - Online trajectory prediction and planning for social robot navigation, In: *IEEE International Conference on Advanced Intelligent Mechatronics (AIM)*, 2017, pp. 1255-1260.
26. <http://cc-smart.net/vi/san-pham/dcmp500.html>
27. <http://cc-smart.net/vi/san-pham/msdah.html>
28. Quigley M., Gerkey B., Conley K., Faust J., Foote T., Leibs J., Berger E., Wheeler R., and A. Ng. - ROS: An open-source Robot Operating System, In: *ICRA Workshop on Open Source Software*, Vol. 32, 2009, pp. 151-170.
29. http://wiki.ros.org/teb_local_planner
30. <http://youtu.be/4RDPuzZglN0>
31. Alahi A., Goel K., Ramanathan V., Robicquet A., Fei-Fei L., and Savarese S. - Social LSTM: Human trajectory prediction in crowded spaces, *IEEE Conference on Computer Vision and Pattern Recognition*, June 2016, pp. 961-971.
32. Rudenko A., Palmieri L., Herman M., Kitani K. M., Gavrila D. M., and Arras K. O. - Human motion trajectory prediction: A survey, <https://arxiv.org/abs/1905.06113v3>, 2019.